

# Nanosphere Lithography as a Versatile Method to Generate Surface-Imprinted Polymer Films for Selective Protein Recognition

Júlia Bognár, Júlia Szűcs, Zsanett Dorkó, Viola Horváth, and Róbert E. Gyurcsányi\*

A versatile approach based on nanosphere lithography is proposed to generate surface-imprinted polymers for selective protein recognition. A layer of 750 nm diameter latex bead-protein conjugate is deposited onto the surface of gold-coated quartz crystals followed by the electrosynthesis of a poly(3,4-ethylenedioxythiophene)/poly(styrenesulfonate) (PEDOT/PSS) film with thicknesses on the order of the bead radius. The removal of the polymer bead-protein conjugates, facilitated by using a cleavable protein-nanosphere linkage is shown to result in 2D arrays of periodic complementary size cavities. Here it is demonstrated by nanogravimetric measurements that the imprinting proceeds further at molecular level and the protein (avidin) coating of the beads generates selective recognition sites for avidin on the surface of the PEDOT/PSS film. The binding capacity of such surface-imprinted polymer films is ca. 6.5 times higher than that of films imprinted with unmodified beads. They also exhibit excellent selectivity against analogues of avidin, i.e., extravidin, streptavidin, and neutravidin, the latter being in fact undetectable. This methodology, if coupled with properly oriented conjugation of the macromolecular template to the nanoparticles, offers the possibility of site-directed imprinting.

## 1. Introduction

Molecular imprinting is a generic method to generate materials with “molecular memory” by performing generally a polymerization of suitable functional monomers in the presence of a target molecule acting as a template.<sup>[1]</sup> A preassembly of the functional monomers and template, which is then conserved by the polymerization reaction, results in the formation of binding sites for the target in the polymeric matrix. Such molecularly imprinted polymers (MIPs) received much attention due to their applicability for separation,<sup>[2]</sup> catalysis,<sup>[1b,3]</sup> sensing<sup>[4]</sup> and drug delivery.<sup>[5]</sup> However, molecular imprinting is still facing

challenges in terms of selective biomacromolecular recognition<sup>[6]</sup> that would fully enable generating synthetic antibodies<sup>[7]</sup> for analytical applications. Despite of the obvious need for robust selective synthetic receptors/sorbents for biomacromolecules it was reported that less than 2% of the MIP literature involves aspects of macromolecular imprinting.<sup>[8]</sup> This reflects difficulties in imprinting large, delicate biomolecules and the conceptual changes that this implies.

The bulk synthesis method, with excellent results in generating MIPs for recognition of low-molecular-weight compounds, is hardly applicable to macromolecules due to their hindered mobility in the highly reticulated polymeric networks. Therefore, the essential prerequisite of generating macromolecular imprints clearly should be to create accessible binding sites amenable for free target exchange between the MIP and the sample phase, i.e., to have binding sites confined to the surface of the MIPs. For

high binding capacities the surface localization of the binding sites should be combined with fabrication methods leading to high surface area/volume ratios of the respective MIPs. Therefore, generation of polymeric micro- and nanostructures comes as a natural necessity to take full advantage of the surface-imprinted sites. This goal is already achieved by protein imprinting of nanometer thin polymer films,<sup>[9]</sup> but more sophisticated methods including microcontact printing with protein modified stamps,<sup>[10]</sup> and using immobilized templates or sacrificial materials<sup>[11]</sup> were also reported. The stamping approach proved to be especially successful in imprinting cells,<sup>[12]</sup> viruses<sup>[13]</sup> and most recently with particles previously imprinted with anti-insulin antibodies to generate insulin binding antibody replicas.<sup>[14]</sup>

The structural and conformational sensitivity<sup>[8,15]</sup> as well as the solubility of biomacromolecules are further reasons why the simple extrapolation of the well-established MIP fabrication technologies for low-molecular-weight compounds is not straightforward. The imprinting of biomacromolecules requires mild conditions and it is generally restricted to aqueous environment. In contrast, low-molecular-weight compounds are typically imprinted in aprotic organic solvents as otherwise

J. Bognár, Z. Dorkó, Prof. R. E. Gyurcsányi  
Department of Inorganic and Analytical Chemistry  
Budapest University of Technology and Economics  
Szt. Gellért tér 4, Budapest, H-1111, Hungary  
E-mail: robertgy@mail.bme.hu

J. Szűcs, Dr. V. Horváth, Prof. R. E. Gyurcsányi  
Research Group for Technical Analytical Chemistry  
Hungarian Academy of Sciences  
Szt. Gellért tér 4, Budapest, H-1111, Hungary



DOI: 10.1002/adfm.201300113

the hydrogen bonding interactions largely contributing to the affinity of MIPs are suppressed by competition from water molecules. Other intrinsic properties of biomacromolecules such as their surface variability in terms of local charge density and hydrophobicity also contribute to the difficulty in providing proper macromolecular imprints. Due to the latter there is an increased likeliness of nonspecific interactions between macromolecules rich in functionality and MIPs, which can easily lead to poor selectivity and cross-reactivity. Epitope imprinting which involves the use of only a fragment of the original macromolecular target for imprinting<sup>[16]</sup> was introduced among others as a means to restrict the imprinting to a targeted sequence and by that to reduce cross-reactivity. Further strategies involved close mimicking of the naturally occurring interactions by using monomers with functionalities already known to interact specifically with the target molecule, e.g., boronic acid-diol,<sup>[17]</sup> metal coordination assisted<sup>[18]</sup> and enzyme-inhibitor interactions.<sup>[19]</sup>

In principle, surface imprinting is inherently advantageous to minimize non-specific interactions because it reduces the contact area between macromolecular targets and bulk polymeric material. Therefore, previously we introduced new methods based on sacrificial polycarbonate microreactors the inner wall of which was modified with proteins by simple physisorption to generate surface-imprinted polymer (SIP) micro-rods<sup>[20]</sup> and microbands.<sup>[21]</sup> Here we propose a versatile concept that enables site-directed protein imprinting and has the potential of downscaling to the low nanometer scale.

The new concept is based on the use of nanosphere lithography with protein-polymer bead conjugates for molecular surface imprinting as shown in **Figure 1**.

In contrast to free protein imprinting, the conjugation of the protein target to a solid surface makes possible its oriented immobilization. In this model study we demonstrate this concept by immobilizing avidin (Av) through its biotin binding

sites by using a heterobifunctional crosslinker, succinimidyl-2-(biotinamido)ethyl-1,3-dithiopropionate (NHS-SS-Biotin). The beads were deposited by drop casting onto the surface of gold-coated quartz crystal resonators and the generated inter-bead voids were filled with polymeric material by electropolymerization of 3,4-ethylenedioxythiophene (EDOT) from an aqueous solution comprising also poly(styrenesulfonate) (PSS, MW: 70 kDa). As such, the electropolymerization could be performed in mild condition compatible with the protein target with the polymerization process being readily controllable by monitoring the current. The choice of PEDOT was motivated by its inherently high biocompatibility<sup>[22]</sup> due to structure similarity with natural compounds such as melanin<sup>[23]</sup> and its electrical conduction. The duration of the electropolymerization was adjusted to grow PEDOT/PSS layers with thicknesses on the order of the radius of the deposited beads. Dissolving away the beads resulted in complementary cavities the interior of which was expected to bear the molecular imprint of the avidin molecules surrounding the respective beads. Here we show the proof of concept that indeed such recognition sites are generated on the surface of the PEDOT/PSS film by using quartz crystal microbalance (QCM) based nanogravimetric measurements.

## 2. Results and Discussion

### 2.1. Deposition of Beads onto the Surface of Gold-Coated Quartz Crystals

While nanosphere lithography is a widely known technique to generate periodic patterns its application is very much focused on fabrication of plasmonic structures<sup>[24]</sup> and according to our best knowledge its use for generating molecular imprints of proteins has never been explored. Remarkably, also the self-assembly of protein modified nanospheres on solid surfaces has little antecedents except studies focused on depositing protein-modified beads within arrays of microwells<sup>[25]</sup> or planar surfaces<sup>[26]</sup> with the aim to increase the local receptor density in bioassay applications. The first step to generate SIPs by nanosphere lithography involved the deposition of Av-modified beads on the planar gold surface of a 10 MHz quartz crystal resonator in as compact layer as possible. Obviously, a compact layer is desirable as it maximizes the imprinted fraction of the polymer surface, however, it should be emphasized that contingent defects in the layer are not as critical for the molecular imprinting process as they are for optical device fabrication.

The Av-conjugated beads were prepared using a cleavable crosslinker (NHS-SS-Biotin) in two successive steps, i.e., first the linker was reacted with the amino surface functionality of the bead and after removing the excess of reagent by centrifugation the Av was linked to the bead through its biotin binding site. The procedure was optimized in terms of the excess of Av required to avoid bead crosslinking. The modification with Av having a pI of ca. 10.5 resulted in a significant shift of the zeta potential of the aliphatic amine modified beads to more positive, i.e., from  $-29.6$  mV to  $+6.7$  mV. Please note that surface pKa of aliphatic amino groups can be as low as 4–4.5<sup>[27]</sup> compared to 9–10 in bulk solution phase and for comparison carboxylated beads had

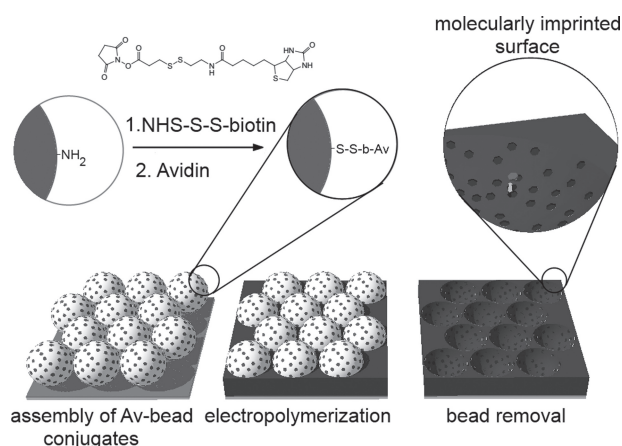


**Figure 1.** Electro-synthesis of surface-imprinted polymer films by nanosphere lithography for selective recognition of avidin (Av). The Av-modified beads are deposited on the surface of an electrode followed by the electropolymerization of EDOT in the presence of PSS. The removal of the beads in two successive steps, i.e., removal of Av by cleaving the disulfide bond of the crosslinker and dissolution of the polymeric bead, leaves behind cavities bearing the imprint of Av molecules.

a zeta potential of  $-73.3$  mV. The use of the cleavable crosslinker was preferred because, unlike beads with COOH and  $\text{NH}_2$  surface functionality that dissolved practically instantaneously in toluene, the removal of avidin-coated particles by the same procedure was found to leave, in some cases, organic residue on the surface. However, this could be effectively avoided if prior to dissolving away the beads the avidin coating was removed by reducing the disulfide bridge of the crosslinker using 50 mM tris(2-carboxyethyl)phosphine (TCEP). Both the successful modification of the beads with protein and their removal from the polymer film were confirmed by hyperspectral optical microscopy using fluorescently labeled avidin (avidin-FITC) modified polystyrene particles (Figure S1, Supporting Information).

While the surface arrangement of colloidal particles<sup>[24b],[28]</sup> can be performed in a variety of ways, given the inherent fragility of the protein layers we used simple drop casting of an aqueous bead suspension.<sup>[29]</sup> The assembly of beads under these conditions is based on the cooperative effect of evaporation driven convection and capillary forces.<sup>[30]</sup> Generating compact hexagonal monolayers of submicron diameter beads bearing carboxylate and amine functionalities proved to be straightforward. However, the arrangement of Av-modified beads required thorough optimization in terms of experimental conditions to result in an optimal bead concentration of 0.13% and deposited amount of  $8.98 \times 10^8$  particles  $\text{cm}^{-2}$ . This corresponds to approximately four times the amount required for a compact monolayer to account for the fraction of particles inherently expended to multilayer formation predominantly at the edge of the demarked surface. The compactness of the layers was most significantly improved by subjecting the surface to UV generated ozone cleaning just prior to the drop casting of the bead suspension and using a silicone rubber ring for the localization of the deposited droplet. Even so the array of Av-modified beads was inherently less uniform and compact than those assembled from unmodified beads. A typical scanning electron micrograph of latex and Av-modified bead layers is shown in Figure 2. Defects in the latex bead monolayers were found to coincide with the occurrence of larger particles present in the commercial bead suspension.

The reason for the deviation of the protein modified beads from a compact hexagonal structure is likely to be caused by the adhesion of these beads to the gold surface, which may prohibit their free movement and ordering during the evaporation of the solvent.

## 2.2. Synthesis of the Surface-Imprinted PEDOT/PSS Film

The voids between the deposited nanospheres were filled by potentiostatically growing a film of PEDOT/PSS from an aqueous solution of EDOT (10 mM) in the presence of PSS at 0.9 V (vs Ag/AgCl). The polymer layer thickness was optimized to obtain maximum imprinted to non-imprinted surface ratio, which based on simple geometrical calculations and assuming uniform growth of the film corresponds to approximately the half-height of the beads (375 nm). The optimal experimental conditions for the film synthesis were determined empirically. Films of different thicknesses were prepared by controlling the electrical charge injected during the polymerization and examining the patterned polymer layers with atomic

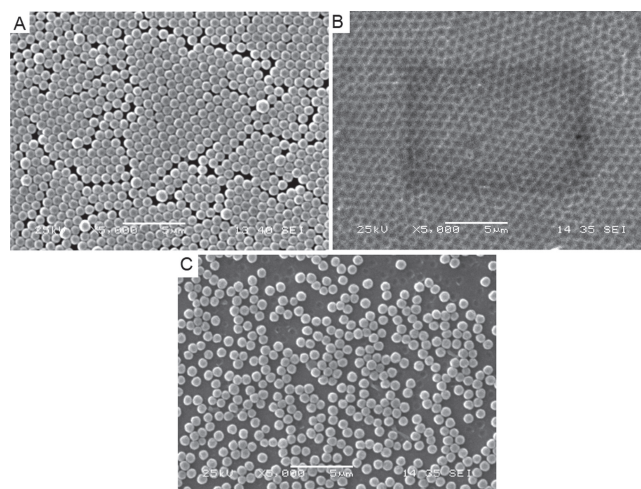


**Figure 2.** Scanning electron micrographs at the same magnification of A) a monolayer of polystyrene beads ( $\phi = 750$  nm) drop casted onto the surface of the quartz crystal resonator, B) patterned PEDOT/PSS films resulted after electropolymerization and removal of the polystyrene beads, as well as C) partial removal of Av-modified beads revealing both the beads and their imprints in the polymer layer.

force microscopy (AFM) after the dissolution of the beads. As shown in Figure 3, the AFM measurements revealed preferential growth of the PEDOT/PSS film alongside the particles and were also conclusive in terms of local morphology of the generated cavities as a function of the electrical charge used during electropolymerization.

At a charge density of  $7.5 \text{ mC cm}^{-2}$  small cavities with a mean depth of ca. 65 nm were formed, that increased to 270 nm at  $19 \text{ mC cm}^{-2}$ . Also, the diameter of the cavities increased from 270 nm to ca. 590 nm. Higher charge densities of 30 and  $41 \text{ mC cm}^{-2}$  resulted in a gradual enfolding of the bead by the grown polymer film, as shown by the decrease in the exposed diameter of the cavity (490 and 260 nm, respectively) as well by its mean depth (460 and 610 nm, respectively). It must be noted that due to the preferential growth of the polymer at the bead surface the thickness value refers to the immediate vicinity of the bead and it is not the average thickness of the film. A somewhat lower charge density,  $17 \text{ mC cm}^{-2}$ , than that would correspond to radius of the beads was chosen as this ensured better control of the polymer thickness, i.e., was less affected by preferential random growth around the bead.

The dissolution of polymer beads exposed parts of bare gold corresponding to areas where the beads touched the surface is noteworthy. To reduce non-specific binding of the protein to these spots,<sup>[31]</sup> the surface was treated with 1 mM (1-mercaptopundec-11-yl)tetra(ethylene glycol) (HS-TEG) for 30 min prior to the QCM measurements (Figure S2, Supporting Information).

## 2.3. Nanogravimetric Measurements of Av Binding to Surface-Imprinted PEDOT/PSS Films

The surface-imprinted polymer film-modified 10 MHz quartz crystal chips were mounted into a flow cell and after the



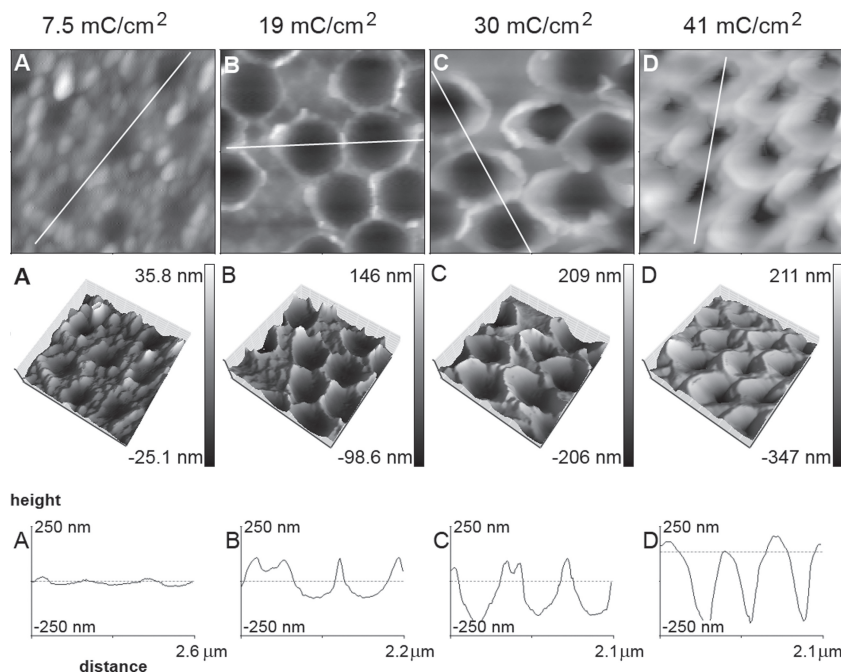


**Figure 3.** AFM images and relevant line scans showing the surface topography of PEDOT/PSS films prepared by nanosphere lithography using 750 nm diameter beads. Scans (A–D) are representative of  $2.2 \mu\text{m} \times 2.2 \mu\text{m}$  areas of patterned PEDOT/PSS films prepared using 7.5, 19, 30, and  $41 \text{ mC cm}^{-2}$  surface charge densities, respectively.

stabilization of the frequency, increasing concentrations of Av were injected in the carrier buffer and the frequency change was monitored in real-time. To determine the effect of the surface imprinting on the binding properties of the polymer the Av binding to non-imprinted polymer film (NIP) was recorded in similar conditions, but in a separate experiment. The NIP films were synthesized in the exact same way as the MIPs but nanospheres that were not modified with Av were used for patterning the PEDOT/PSS film. Typical QCM sensorgrams are shown in **Figure 4**.

We examined the effect of surfactant content in the eluent buffer on the suppression of non-specific adsorption. A non-ionic detergent was used for this purpose as ionic detergents were shown to cause complications in protein MIPs.<sup>[6]</sup> The Av binding to MIP and NIP surfaces was determined at various amounts of Tween-20 added to the carrier buffer. Addition of 0.01% Tween-20 to the Tris-EDTA buffer decreased by half the total amount of avidin bound to the NIP (Figure S3, Supporting Information). Interestingly, concomitantly the bound Av quantity increased significantly on the MIP as compared with the detergent-free Tris-EDTA buffer. Therefore, all further experiments were carried out with Tris-EDTA buffer containing 0.01% Tween-20 as carrier solution. Under this condition at the highest avidin concentration studied the amount of avidin bound on the imprinted surfaces was  $1.34 \mu\text{g cm}^{-2}$  while on the NIP surface  $0.21 \mu\text{g cm}^{-2}$  which accounts for an imprinting factor of 6.5 (**Figure 5**) This value is higher than the vast majority of imprinting factors reported for acrylic polymers (generally between 1.2 and 4.5).<sup>[32]</sup> However, we could not reassert our previous result of  $\approx 10$  obtained with PEDOT/PSS polymer microbands,<sup>[21]</sup> which is in fact close to the maximum

value ever reported for protein MIPs.<sup>[9c]</sup> This is most likely due to the relatively large non-imprinted fraction of the surface as result of the non-compact Av-modified bead layer.

The selectivity of Av-imprinted polymers was determined for three avidin species: ExtrAvidin (EA), NeutrAvidin (NA), and Streptavidin (SA); all of them having a near-neutral isoelectric point (EA: 6.5, NA: 6.3, SA: 5.5) and various degrees of structural similarity with avidin. ExtrAvidin and NeutrAvidin are deglycosylated forms of avidin, while Streptavidin is a biotin-binding protein found in the bacterium *Streptomyces avidinii* with only 33% of the amino acid residues identical to those found in Av.<sup>[33]</sup> The selectivity study further included Lysozyme (Lys), representative for high isoelectric point (pI) proteins and bovine serum albumin (BSA) with widely different pI, but similar molecular weight. The respective proteins were injected at a concentration of  $0.1 \text{ mg mL}^{-1}$  and the amount of protein bound to MIP and NIP surfaces was determined by QCM. The surface was regenerated between measurements with 1 M NaCl. The Av-imprinted PEDOT/PSS film showed clearly the greatest affinity for Av, followed in order by Lys, BSA

and the avidin-analogues (**Figure 6**). The significant Lys adsorption is not surprising as it is one of the most surface active proteins that can form multilayer aggregates upon adsorption to charged surfaces.<sup>[34]</sup> The relatively high amount of adsorbed Lys having a pI of 11.4 suggests that electrostatic interactions play an important role in the recognition process. However, the Lys adsorption is practically the same on both MIP and NIP surfaces and also similar to the Av adsorption on the NIP, which

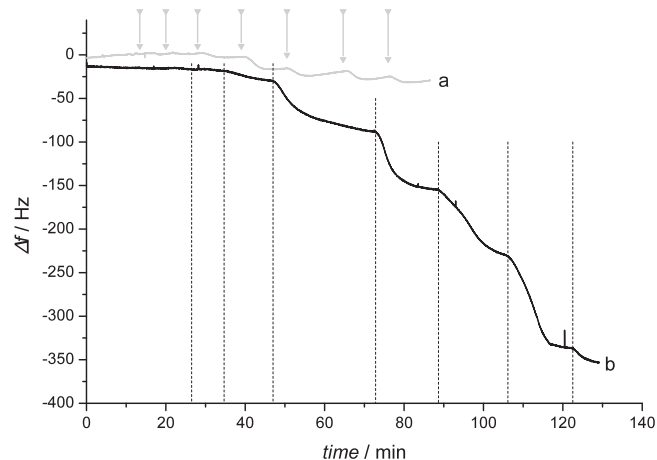


**Figure 4.** Frequency response recorded during Av binding to a) NIP and b) Av-imprinted polymer.  $250 \mu\text{L}$  Av solutions of the following concentrations were injected successively in the carrier solution flown at a rate of  $60 \mu\text{L min}^{-1}$ :  $10^{-3}$ ,  $10^{-2}$ ,  $2 \times 10^{-2}$ ,  $5 \times 10^{-2}$ ,  $10^{-1}$ ,  $2 \times 10^{-1}$ , and  $3 \times 10^{-1} \text{ mg mL}^{-1}$ . Injection instances are marked with dashed lines for MIP and arrows for NIPs.

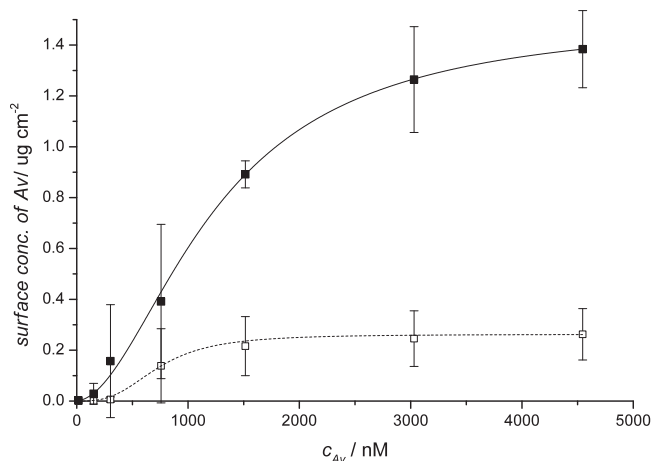


**Figure 5.** Binding isotherms of Av to the imprinted (■) and non-imprinted (□) PEDOT/PSS patterns. The data points are the average of measurements performed on three different MIP- and NIP-modified quartz crystals.

suggest inherent adsorption to the non-imprinted PEDOT/PSS material. Given the fivefold increase in the Av adsorption on the MIP as compared with the NIP and Lys adsorption on both MIP and NIP surfaces clearly demonstrates that the Av recognition on NIP cannot be solely attributed to electrostatic interactions.<sup>[35]</sup> A major benefit of the proposed method is the remarkably suppressed adsorption of the avidin analogues on the MIP, most spectacularly of EA, which is even lower than that of BSA and significantly better than in earlier studies using randomly immobilized Av for imprinting.<sup>[21]</sup> The somewhat lower imprinting factor than determined from binding isotherms is due to the effect of the 1 M NaCl solution used for regeneration. It was shown previously that high ionic strength solutions

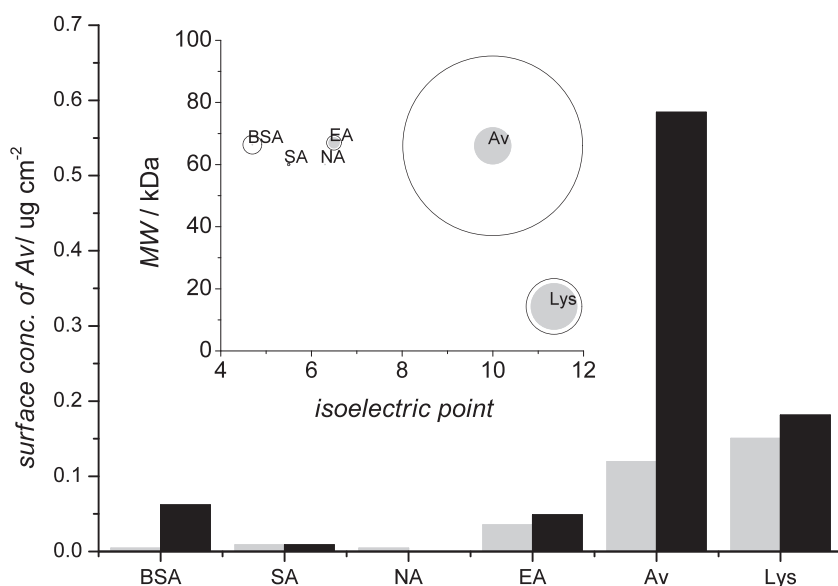


**Figure 6.** Adsorbed protein amounts to Av-imprinted polymer (black) and NIP (grey) for different proteins. The inset compares the pI and molecular weight of the proteins with their adsorbed amount onto the MIP (open black circles) and NIP (filled grey circles); the area of each circle is proportional to the adsorbed protein amount.

are inducing both morphological and composition changes in PEDOT/PSS films.<sup>[36]</sup>

### 3. Conclusions

We have demonstrated that nanosphere lithography can be used to generate surface-imprinted polymers for selective protein recognition. A remarkable selectivity and an imprinting factor close to state of the art were obtained despite of the non-compact nanosphere assembly, which exposes a significant fraction of the non-imprinted surface for interaction. Future work is directed to address this issue as well as the possibility of generating multilayer structures for higher binding capacity surface-imprinted nanostructures. The method proposed has the following potential advantages: (i) the oriented immobilization of the macromolecular template on the nanosphere surface makes feasible site-directed imprinting of the respective macromolecules, (ii) the binding site density on the surface-imprinted polymer can be controlled by adjusting the nanosphere diameter and/or surface density of the protein coating, (iii) the nanosphere carrier offers utmost flexibility in terms of adjusting the local chemical environment of the macromolecular template and imposes less strain on the control of the polymer film thickness as compared with surface-confined direct macromolecular imprinting requiring ultrathin smooth films.<sup>[34]</sup>

### 4. Experimental Section

**Chemicals and Materials:** Monodisperse polystyrene beads of 750 nm diameter with primary amine (Polybead Amino) and carboxyl (Polybead Carboxylate) surface groups were purchased from Polysciences (Warrington, PA, USA). Avidin, NeutrAvidin and the heterobifunctional crosslinker, succinimidyl-2-(biotinamido)ethyl-1,3-dithiopropionate, were obtained from Thermo Fisher Scientific (Rockford, IL, USA). The proteins avidin-FITC, Streptavidin, ExtrAvidin, lysozyme (Lys) and bovine serum albumin (BSA) were obtained from Sigma Aldrich (St. Louis, MO, USA). The buffer components: phosphate buffered saline (PBS, pH 7.4, 10 mM phosphate buffer, 137 mM NaCl, 2.7 mM KCl), Tween containing Tris-EDTA buffer (TET, pH 8.0, 10 mM Tris, 1 mM EDTA, 0.01% Tween 20) as well as the reducing agent tris(2-carboxyethyl)phosphine hydrochloride and (1-mercaptoundec-11-yl) tetra(ethylene glycol) were purchased from Sigma Aldrich. The monomer 3,4-ethylenedioxythiophene and poly(sodium 4-styrenesulfonate) (MW: 70 000 g mol<sup>-1</sup>) were from Sigma Aldrich, dimethyl sulphoxide (DMSO) was purchased from ROMIL (Cambridge, UK). Aqueous solutions were prepared with ultrapure deionized water (DI water, 18 MΩ cm, Millipore Corporation, USA).

**Synthesis of Avidin-Polymer Bead Conjugates:** The Polybead Amino stock solution was diluted 10 times with PBS followed by the addition of NHS-SS-Biotin (100 μL, 10 mM) in DMSO. The suspension was incubated under continuous shaking for 60 min and then centrifuged at 16 660g for 10 min. The supernatant was discarded, and the particles were resuspended in PBS (900 μL). This procedure was repeated five times to separate the biotinylated nanoparticle from the free reagent.

Further modification with Av was made by mixing avidin in PBS (100  $\mu\text{L}$ , 10 mg  $\text{mL}^{-1}$ ) with biotinylated bead suspension (900  $\mu\text{L}$ ) for 60 min. The beads were collected by centrifugation (at 16 660g for 10 min) and washed five times with DI water, followed by resuspension in DI water (1000  $\mu\text{L}$ ) to give a final concentration of ca.  $10^{10}$  particles  $\text{mL}^{-1}$ .

**Preparation and Characterization of Avidin-Imprinted Polymer Film:** The surface of the gold electrode (0.205  $\text{cm}^2$ ) on 10 MHz AT-cut gold-coated quartz crystal resonator (Gamry Instruments, Warminster, PA, USA) was pretreated in a UV ozone cleaner (Novascan PSD Pro UV Ozone System) for 15 min. An aqueous suspension of Av-modified beads (0.13 w/v%) was drop cast onto the surface to provide a calculated surface coverage of  $8.98 \times 10^8$  beads  $\text{cm}^{-2}$  and slowly dried at a controlled relative humidity of 75% ( $T = 23^\circ\text{C}$ ). The potentiostatic deposition of PEDOT/PSS within the voids of the particle array was done at 0.9 V (reference electrode: Ag/AgCl/3M NaCl, counter electrode: Pt) in an aqueous solution of 10 mM EDOT and 25 mM NaPSS. The amount of film deposited (thickness of the layer) was controlled based on the electrical charge passed during the electropolymerization. Before dissolving away the polystyrene beads in toluene the avidin was cleaved from the surface of the beads by reduction of the disulfide bonds with TCEP (50 mM) for 30 min. The quartz crystals were then rinsed with ethanol and DI water, and dried. The bare gold surfaces exposed upon removal of the microspheres were blocked with HS-TEG (1 mM (1-mercaptopoundec-11-yl)tetra(ethylene glycol) in PBS for 30 min) in order to reduce non-specific adsorption. Non-imprinted polymers were prepared in the same way, except that unmodified beads were used. The modification of the beads with Av and their removal from the PEDOT/PSS surface was confirmed by using fluorescent labeled Av (Av-FITC) and a hyperspectral optical imaging system consisting of an Olympus IX71 inverted epifluorescence microscope and a Pariss hyperspectral imaging system (LightForm Inc., Asheville, NC, USA). The fluorescence intensities were recorded in at least 240 different spots on the surface using an LCPLFL20XPH/0.40 long working distance objective and a U-MNB2 fluorescence filter cube (narrow band excitation (470–490 nm), 500 nm cut-off dichroic mirror and a long pass 520 nm emission filter). The morphology of the imprinted surfaces was investigated with an easyScan2 atomic force microscope (Nanosurf AG, Liestal, CH) in dynamic force mode.

**Nanogravimetric Investigation of the Binding Processes:** The MIP- and NIP-coated 10 MHz Au chips were mounted into a flow cell of 120  $\mu\text{L}$  (Als Co. Ltd, Tokyo, Japan) and connected to Gamry eQCM 10M electrochemical quartz crystal microbalance. The protein solutions (250  $\mu\text{L}$ ) were injected into TET carrier solution flown at a rate of 60  $\mu\text{L min}^{-1}$ . The surface concentration of the adsorbed protein was calculated from changes in the resonant frequency using the Sauerbrey equation. Calibrations were carried out by consecutive injections of increasing concentrations of Av solutions, without regenerating the surface between the injections. During the selectivity measurements, the polymer surface was regenerated by injecting 1 M NaCl into the flow cell after each protein adsorption.

## Supporting Information

Supporting Information is available from the Wiley Online Library or from the author.

## Acknowledgements

The financial support of the Hungarian Scientific Fund (K 104724 and NF 69262) is gratefully acknowledged.

Received: January 10, 2013

Revised: February 15, 2013

Published online: April 11, 2013

- [1] a) G. Wulff, W. Vesper, R. Grobe-Einsler, A. Sarhan, *Makromol. Chem.* **1977**, 178, 2799; b) K. J. Shea, E. A. Thompson, S. D. Pandey, P. S. Beauchamp, *J. Am. Chem. Soc.* **1980**, 102, 3149; c) R. Arshady, K. Mosbach, *Makromol. Chem.* **1981**, 182, 687.
- [2] a) A. Beltran, F. Borrell, P. A. G. Cormack, R. M. Marce, *TrAC, Trends Anal. Chem.* **2010**, 29, 1363; b) Y. P. Huang, Z. S. Liu, C. Zheng, R. Y. Gao, *Electrophoresis* **2009**, 30, 155.
- [3] a) R. Müller, L. I. Andersson, K. Mosbach, *Makromol. Chem. Rapid Commun.* **1993**, 14, 637; b) A. G. Strikovsky, D. Kasper, M. Grün, B. S. Green, J. Hradil, G. Wulff, *J. Am. Chem. Soc.* **2000**, 122, 6295; c) B. Sellergren, R. N. Karmalkar, K. J. Shea, *J. Org. Chem.* **2000**, 65, 4009.
- [4] a) S. A. Piletsky, A. P. F. Turner, *Electroanalysis* **2002**, 14, 317; b) O. Y. F. Henry, D. C. Cullen, S. A. Piletsky, *Anal. Bioanal. Chem.* **2005**, 382, 947; c) M. J. Whitcombe, I. Chianella, L. Larcombe, S. A. Piletsky, J. Noble, R. Porter, A. Horgan, *Chem. Soc. Rev.* **2011**, 40, 1547; d) C. Malatesta, E. Mazzotta, R. A. Picca, A. Poma, I. Chianella, S. A. Piletsky, *Anal. Bioanal. Chem.* **2012**, 402, 1827.
- [5] C. Alvarez-Lorenzo, A. Concheiro, *J. Chromatogr. B* **2004**, 804, 231.
- [6] E. Verheyen, J. P. Schillemans, M. van Wijk, M. A. Demeinix, W. E. Hennink, C. F. van Nostrum, *Biomaterials* **2011**, 32, 3008.
- [7] K. Haupt, K. Mosbach, *Trends Biotechnol.* **1998**, 16, 468.
- [8] D. R. Kryscio, N. A. Peppas, *Acta Biomater.* **2012**, 8, 461.
- [9] a) Z. H. Zhang, Y. M. Long, L. H. Nie, S. Z. Yao, *Biosens. Bioelectron.* **2006**, 21, 1244; b) T. Shiomi, M. Matsui, F. Mizukami, K. Sakaguchi, *Biomaterials* **2005**, 26, 5564; c) A. Bossi, S. A. Piletsky, E. V. Piletska, P. G. Righetti, A. P. F. Turner, *Anal. Chem.* **2001**, 73, 5281.
- [10] a) H. Y. Lin, C. Y. Hsu, J. L. Thomas, S. E. Wang, H. C. Chen, T. C. Chou, *Biosens. Bioelectron.* **2006**, 22, 534; b) Y.-W. Chen, J. Rick, T. C. Chou, *Org. Biomol. Chem.* **2009**, 7, 488.
- [11] a) Y. Li, H. H. Yang, Q. H. You, Z. X. Zhuang, X. R. Wang, *Anal. Chem.* **2006**, 78, 317; b) A. Nematollahzadeh, W. Sun, C. S. A. Aureliano, D. Lütkemeyer, J. Stute, M. J. Abdekhodaie, A. Shojaei, B. Sellergren, *Angew. Chem. Int. Ed.* **2011**, 50, 495.
- [12] a) C. Alexander, E. N. Vulfson, *Adv. Mater.* **1997**, 9, 751; b) O. Hayden, K. J. Mann, S. Krassnig, F. L. Dickert, *Angew. Chem. Int. Ed.* **2006**, 45, 2626.
- [13] F. L. Dickert, O. Hayden, R. Bindeus, K. J. Mann, D. Blaas, E. Waigmann, *Anal. Bioanal. Chem.* **2004**, 378, 1929.
- [14] R. Schirhagl, U. Latif, D. Podlipna, H. Blumenstock, F. L. Dickert, *Anal. Chem.* **2012**, 84, 3908.
- [15] N. W. Turner, X. Liu, S. A. Piletsky, V. Hlady, D. W. Britt, *Biomacromolecules* **2007**, 8, 2781.
- [16] A. Rachkov, N. Minoura, *Biochim. Biophys. Acta-Protein Struct. Molec. Enzym.* **2001**, 1544, 255.
- [17] M. Glad, O. Norrlöw, B. Sellergren, N. Siegbahn, K. Mosbach, *J. Chromatogr. A* **1985**, 347, 11.
- [18] a) F. H. Arnold, *Nat. Biotechnol.* **1991**, 9, 151; b) M. Kempe, M. Glad, K. Mosbach, *J. Mol. Recognit.* **1995**, 8, 35.
- [19] A. A. Vaidya, B. S. Lele, M. G. Kulkarni, R. A. Mashelkar, *J. Appl. Polym. Sci.* **2001**, 81, 1075.
- [20] A. Menaker, V. Syritski, J. Reut, A. Opik, V. Horváth, R. E. Gyurcsányi, *Adv. Mater.* **2009**, 21, 2271.
- [21] G. Lautner, J. Kaev, J. Reut, A. Opik, J. Rappich, V. Syritski, R. E. Gyurcsányi, *Adv. Funct. Mater.* **2011**, 21, 591.
- [22] S. M. Richardson-Burns, J. L. Hendricks, B. Foster, L. K. Povlich, D.-H. Kim, D. C. Martin, *Biomaterials* **2007**, 28, 1539.
- [23] D. C. Martin, *Nat Mater* **2007**, 6, 626.
- [24] a) C. L. Haynes, R. P. Van Duyne, *J. Phys. Chem. B* **2001**, 105, 5599; b) X. Y. Zhang, A. V. Whitney, J. Zhao, E. M. Hicks, R. P. Van Duyne, *J. Nanosci. Nanotechnol.* **2006**, 6, 1920.
- [25] a) Y. Zhang, *Colloids Surf., B* **2006**, 48, 95; b) C. Wang, Y. Zhang, H. S. Seng, L. L. Ngo, *Biosens. Bioelectron.* **2006**, 21, 1638.

- [26] J. R. Li, G. C. Henry, J. C. Garno, *Analyst* **2006**, 131, 244.
- [27] D. V. Vezenov, A. Noy, L. F. Rozsnyai, C. M. Lieber, *J. Am. Chem. Soc.* **1997**, 119, 2006.
- [28] N. Vogel, C. K. Weiss, K. Landfester, *Soft Matter* **2012**, 8, 4044.
- [29] N. D. Denkov, O. D. Velev, P. A. Kralchevsky, I. B. Ivanov, H. Yoshimura, K. Nagayama, *Nature* **1993**, 361, 26.
- [30] P. A. Kralchevsky, K. Nagayama, *Langmuir* **1994**, 10, 23.
- [31] a) G. Lautner, Z. Balogh, V. Bardóczy, T. Meszáros, R. E. Gyurcsányi, *Analyst* **2010**, 135, 918; b) K. L. Prime, G. M. Whitesides, *J. Am. Chem. Soc.* **1993**, 115, 10714.
- [32] a) Q. Q. Gai, F. Qu, Z. J. Liu, R. J. Dai, Y. K. Zhang, *J. Chromatogr. A* **2010**, 1217, 5035; b) W. X. Su, J. Rick, T. C. Chou, *Microchem. J.* **2009**, 92, 123; c) A. Cutivet, C. Schembri, J. Kovensky, K. Haupt, *J. Am. Chem. Soc.* **2009**, 131, 14699; d) A. Nematollahzadeh, W. Sun, C. S. A. Aureliano, D. Lutkemeyer, J. Stute, M. J. Abdekhodaie, A. Shojaei, B. Sellergren, *Angew. Chem. Int. Ed.* **2011**, 50, 495.
- [33] M. D. Savage, G. Mattson, S. Desai, G. W. Nielander, S. Morgensen, E. J. Conklin, *Avidin-biotin Chemistry. A Handbook*, Pierce Chemical Co, Rockford, IL **1992**.
- [34] D. Dechtrirat, K. J. Jetzschmann, W. F. M. Stöcklein, F. W. Scheller, N. Gajovic-Eichelmann, *Adv. Funct. Mater.* **2012**, 22, 5231.
- [35] Z. Chai, H. Chen, J. Kong, Y. Wang, G. Fu, *J. Chromatogr. B* **2011**, 879, 669.
- [36] Y. Xia, J. Ouyang, *Macromolecules* **2009**, 42, 4141.